Origin and evolution of photoluminescence from Si nanocrystals embedded in a SiO_2 matrix

X. X. Wang,[1,*] J. G. Zhang,[1] L. Ding,[2] B. W. Cheng,[1] W. K. Ge,[2] J. Z. Yu,[1] and Q. M. Wang[1]
[1]*State Key Laboratory of Integrated Optoelectronics, Institute of Semiconductors, Chinese Academy of Sciences, Beijing, 100083, China*
[2]*Department of Physics, Hong Kong University of Science and Technology, Hong Kong, China*
(Received 17 May 2005; revised manuscript received 22 July 2005; published 9 November 2005)

A detailed analysis of the photoluminescence (PL) from Si nanocrystals (NCs) embedded in a silicon-rich SiO_2 matrix is reported. The PL spectra consist of three Gaussian bands (peaks A, B, and C), originated from the quantum confinement effect of Si NCs, the interface state effect between a Si NC and a SiO_2 matrix, and the localized state transitions of amorphous Si clusters, respectively. The size and the surface chemistry of Si NCs are two major factors affecting the transition of the dominant PL origin from the quantum confinement effect to the interface state recombination. The larger the size of Si NCs and the higher the interface state density (in particular, Si=O bonds), the more beneficial for the interface state recombination process to surpass the quantum confinement process, in good agreement with Qin's prediction in Qin and Li [Phys. Rev. B **68**, 85309 (2003)]. The realistic model of Si NCs embedded in a SiO_2 matrix provides a firm theoretical support to explain the transition trend.

DOI: 10.1103/PhysRevB.72.195313 PACS number(s): 78.67.Bf

I. INTRODUCTION

The discovery of visible photoluminescence (PL) from electrochemically etched porous silicon (PS) at room temperature has stimulated extensive research in the development of nanostructured Si materials and in the exploration of the underlying luminescence mechanism in order to realize an efficient Si-based light emitter.[1] Low-dimensional Si materials such as surface-oxidized Si nanocrystals (NCs), Si/SiO_2 multilayers or superlattices, and Si NCs embedded in a Si-rich oxide matrix (SRO) are produced with different techniques[2–6] to overcome the problem of chemical and mechanical instability of PS. As to the widely debated luminescence mechanism, the recent consensus is that both the quantum confinement effect and the interface state recombination play important roles. It seems to be well established that the PL peak energy varies with the size of Si nanostructures in the quantum confinement scheme, while the interface state emission is generally regarded to be size insensitive.[7,8] Well-characterized Si NCs[7] and two-dimensional quantum well structures[8] easily provide experimental evidences that both core and interfacial emission centers contribute to the red and infrared PL by varying the size of Si NCs or the thickness of Si layers. Nevertheless, it is still a very difficult task to separate the interfacial effect from the quantum confinement effect in the radiative emission from the complex-structured SRO material system due to the lack of the effective size control of Si NCs and their broad size distribution. Thus, such references are scarce.[9] On the other hand, the interfacial radiative states are presumed to play a key role in the population inversion mechanism of the SRO material system in the four-level recombination gain model.[10] Hence the nature and the properties of the interface states have become crucial in order to verify this model.

Regarding the interface state effect as a function of Si NC size, there also seems to be controversial conclusions. In Ref. 11, it is considered that the quantum confinement effect dominates in NCs with larger sizes, while for NCs with smaller sizes the interface state effect plays a key role. Contrarily, Qin and Li regard that there is a critical NC size, below which the quantum confinement effect dominates, and above which the interface state effect prevails.[12] Widely varied synthesis processes might be the reason for the different explanations of the origin of Si NCs' luminescence. The former model is supported by the observations in the cases of porous silicon quantum dots after exposure to oxygen[11] and controlled passivation of isolated Si NCs.[13] However, few experimental results are reported to support Qin and Li's model.

In this paper, studies are carried out to separate the contribution of interfacial state recombination from Si NC's band edge emission in the PL spectra of SRO. The relative contribution of interface state radiative emission to PL as a function of Si atomic content in SRO and subsequent annealing treatment is also investigated. Our results indicate that the larger the size of Si NCs, the higher the interface state density, and the more the interface state recombination process dominates over the quantum confinement process in the SRO material system, in support of Qin and Li's model.

The paper is organized as follows. A brief description of the fabrication technique and characterization measurements of the SRO material system is given in Sec. II. The complete study of the PL behavior is presented in Sec. III. First the study is carried out to separate the contribution of the interface state recombination from Si NC's band edge emission in the PL spectra (Sec. III A), then the effect of the size and surface chemistry of Si NC on the transition of dominant PL origin is considered (Sec. III B). The transition mechanism of the two PL origins is discussed in Sec. IV. Finally in Sec. V conclusions are presented.

II. EXPERIMENT

Amorphous SiO_x $(0<x<2)$ films were deposited by plasma-enhanced chemical-vapor deposition (PECVD) technique from appropriate gaseous mixtures of 15% argon-diluted silane and nitrous oxide, in a capacitively coupled

 ©2005 The American Physical Society

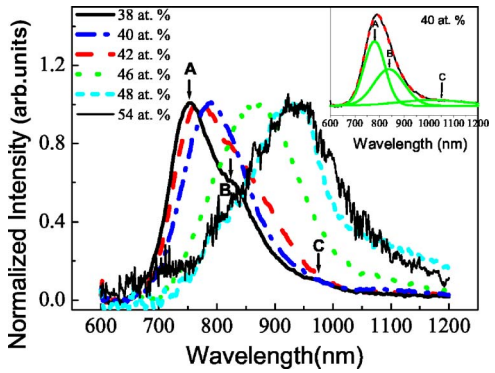

FIG. 1. (Color online) A comparison of room-temperature PL spectra of samples with different Si concentration annealed at 1150 °C for 1 h in N_2 ambient (300 SCCM). The inset is the Gaussian deconvolution of the PL spectrum of 40 at. % Si sample. The approximate positions of peak *A*, *B*, and *C* are denoted by arrows in the figure and its inset.

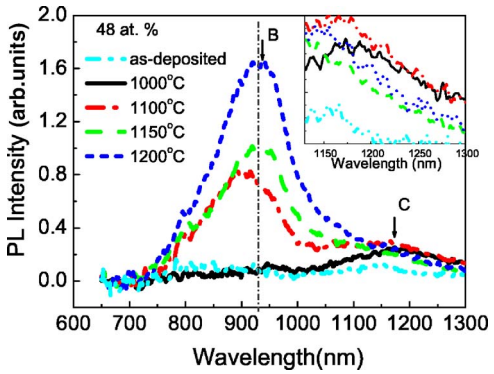

FIG. 2. (Color online) A comparison of room-temperature PL spectra of 48 at. % Si sample annealed at different temperatures for 1 h in N_2 ambient (300 SCCM). The approximate positions of peaks *B* and *C* are denoted by arrows. The inset is the enlargement of the PL spectra in the wavelength range from 1130 nm to 1300 nm.

reactor with a constant deposition pressure of 110 mTorr. The substrate was the phosphorous-doped Si (100) wafer with a resistivity of 3–6 Ω cm. Before loading into the chamber, Radio Corporation of America (RCA) cleaning and hydrofluoric acid (HF) dip procedures were applied to clean the wafer surface. The substrate was heated to 200 °C and the radio frequency (13.56 MHz) power was kept at 50 W. The flow rate ratio Γ ($[SiH_4]/[N_2O]$) varied between 3.5 and 12. The deposition time was 30 min to obtain about 300 nm thick films. With this procedure, the Si concentration of SiO_x films ranged from 38 at. % to 54 at. %, determined by Rutherford backscattering spectrometry (RBS). After the deposition, SiO_x films were annealed for 60 min between 900 °C and 1200 °C in ultrapure N_2, O_2, or Ar gases to form Si NCs. Hydrogen passivation of SRO films was subsequently achieved by annealing at 500 °C for 1 h in the forming gas of 95% N_2 and 5% H_2. The structural properties were characterized by employing Fourier transform infrared spectra (FTIR), Raman spectroscopy and cross-sectional high resolution transmission electron microscopy (HRTEM).

PL measurements were performed using the 488 nm line of Ar^+ pumping laser. The room-temperature PL signals were detected by a liquid nitrogen-cooled Ge detector and the excitation power was fixed at 40 mW over a circular area of about 1 mm in diameter at the Institute of Semiconductors. The temperature-dependent PL signals were probed by a combination of a photomultiplier tube PMT928 and a liquid nitrogen-cooled Ge detector, and the excitation power was 30 mW at the Hong Kong University of Science and Technology. All PL spectra were corrected for the detector spectral response.

III. RESULTS

A. Origin of the photoluminescence

Typical SRO samples emit light at room temperature in a broad red and infrared range of 700 to ~1100 nm. Figure 1 compares the PL spectra of SRO samples with different Si content annealed at 1150 °C for 1 h in ultrapure N_2 ambient. In order to show the shift of the peak wavelength clearly, all spectra are normalized so that the peak intensity is unity for all samples. It appears that the peak position has a marked redshift with the increase of the average Si NC size resulting from higher Si concentration, as expected by the quantum confinement model.[6] However, the spectrum of 38 at. % Si sample actually consists of three obvious peaks, indicated by the arrows in Fig. 1. Moreover, other PL spectra are also comprised of three Gaussian bands with different relative intensity, named peaks *A*, *B*, and *C* respectively. As an example, the inset of Fig. 1 shows the deconvolution of PL spectrum of the 40 at. % Si sample. The peak positions of three Gaussian bands are observed to vary as a function of Si concentration, i.e., *A* is peaked between 750–800 nm, *B* 850–950 nm, and the weak, broad *C* around 1000–1150 nm.

Firstly, the origin of peak *C* is investigated. Figure 2 shows the thermal annealing effect on the PL of 48 at. % Si sample. Peak *C* is present in the as-deposited film, increases and reaches the maximum at 1100 °C annealing temperature, and then decreases with further increase of the annealing temperature. The same SRO film (48 at. % Si) deposited on a quartz substrate is used to carry out Raman spectrometry in order to eliminate the signal from the Si substrate (Fig. 3). It's well known that few amorphous Si (α-Si) clusters exist in as-deposited films and the first stage of phase separation of Si and SiO_2 in a SiO_x matrix begins at 900 °C, but well-defined α-Si clusters are formed only at 1000 °C.[14] The peaks corresponding to the modes of α-Si (indicated by arrows in Fig. 3) can be identified in Raman spectra[15] of the sample annealed at 1000 °C. The sharp transverse optical (TO) mode of Si NCs (513 cm^{-1}) superimposed on the broad α-Si modes indicates the nucleation and growth of Si NCs after the phase separation. With the increase of the annealing temperature up to 1150 °C, the transverse optical TO mode signal of Si NCs dramatically increases and becomes narrower due to enhanced crystallization. On the other hand, α-Si modes decrease markedly at 1150 °C, owing to the crystallization of α-Si clusters. Note that the variation of the amount of α-Si clusters based on Raman results is similar to the trend of peak *C* emission intensity as a function of the annealing temperature, suggesting that the broad peak *C* is

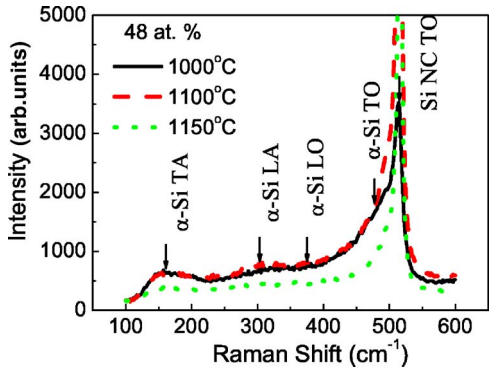

FIG. 3. (Color online) Raman spectra of 48 at. % Si SRO film grown on quartz substrate annealed at 1000 °C, 1100 °C, and 1150 °C for 1 h in N_2 ambient (300 SCCM). 150, 300, 380, and 480 cm^{-1} (indicated by arrows) are ascribed to transverse acoustic (TA), longitudina1 acoustic (LA), longitudinal optical (LO), transverse optical (TO) modes of α-Si, respectively. The peak at 513 cm^{-1} is ascribed to TO mode of Si NCs.

related to α-Si clusters. Moreover, Fig. 1 demonstrates that the relative intensity of the tail at longer wavelength ($>$1000 nm) increases with the Si content. Since SRO films with higher Si content contain more α-Si clusters, this observation further supports the opinion that peak *C* is ascribed to localized state transitions in α-Si clusters[16] in the SRO material system.

In the following part, attention is focused on the origins of peaks *A* and *B*. Figures 4(a) and 4(b) show the peak intensity ratio of peak *A* to *B* and the peak position of PL spectra at the annealing temperatures of 1150 °C and 1200 °C, respectively. In the case of 1150 °C annealing, the peak intensity ratio of *A* to *B* decreases from 1.8 to 0.35 as the Si content increases from 38 to 46 at. %, indicating a dominant peak transition from *A* to *B*. Correspondingly, the peak position jumps from ~750 nm to ~860 nm. Therefore, the significant redshift of PL peak position as the Si content increases is mainly due to a dominant peak transition from *A* to *B*. As is shown in Fig. 4(b), we notice that for the samples dominated by peak *A* emission at 1150 °C annealing (e.g., 38 and 40 at. % Si), there is also a dominant peak transition from *A* to *B* and correspondingly a large redshift (50–70 nm) of peak position when the annealing temperature increases to 1200 °C. On the other hand, for the samples dominated by peak *B* emission at 1150 °C annealing, only a very small redshift (less than 10 nm) in the peak position is observed (an example of this case is shown in Fig. 2, with 48 at. % Si), and the peak intensity ratio of *A* to *B* varies only slightly. Hence, the annealing temperature-induced redshift is also mainly due to the dominant peak transition from *A* to *B*. As can be seen in Figs. 4(a) and 4(b), such transition happens suddenly in a narrow composition (42–44 at. % Si) or annealing temperature range (1150 to ~1200 °C), leading to a jump in the peak's redshift, in contrast to the gradual peak shift expected in the quantum confinement scheme. It is interesting to note that in Figs. 4(a) and 4(b) peak *B* position does depend on the sample composition, shifting from ~860 nm to ~930 nm and then saturates around 930 nm when the Si composition increases from 46 to 54 at. % under

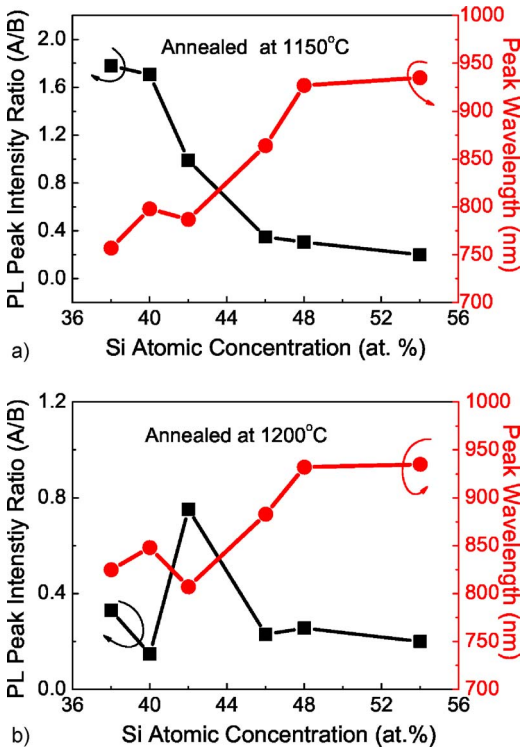

FIG. 4. (Color online) Peak PL intensity ratio of peak *A* to *B* and peak position as a function of Si concentration of SRO films. (a) annealed at 1150 °C for 1 h in N_2 ambient (300 SCCM), (b) annealed at 1200 °C for 1 h in N_2 ambient (300 SCCM). Full square ■: PL intensity ratio, full circle (gray color): peak position.

both annealing conditions. This phenomenon will be discussed in detail in Sec. IV.

In order to clarify the origins of peaks *A* and *B*, we explore in greater detail the difference between the samples dominated by peak *A* (40 at. % Si) and *B* (46 at. % Si) annealed at 1150 °C, named as *S_A* and *S_B* for abbreviation, respectively. The high resolution TEM images clearly demonstrate Si NCs with different orientations exist in both *S_A* and *S_B*. The major difference is the Si NC size and size distribution (standard deviation) of the two samples. The mean diameter of Si NCs is 2.0±0.3 nm in *S_A* and 2.6±0.5 nm in *S_B* by a detailed statistical analysis of the HRTEM.

Temperature-dependent PL spectra from *S_A* and *S_B* are shown in Fig. 5. The appearance of the weak signal around 1.3 μm below 100 K arises from the defect recombination in the Si substrate. The peak position of *S_A* shifts toward longer wavelength when the temperature increases from 10 K to 300 K, while there is a negligible shift in the case of *S_B*. Therefore, it is assumed that peak *A* is related to the quantum confinement of Si NCs, while peak *B* is related to the interface states. For the bulk crystalline Si (*c*-Si), it's well known that the combination of thermal expansion and electron-phonon interaction contributes to the shrinkage of the band gap with the increase of temperature, and it can be fit by the relation[17]

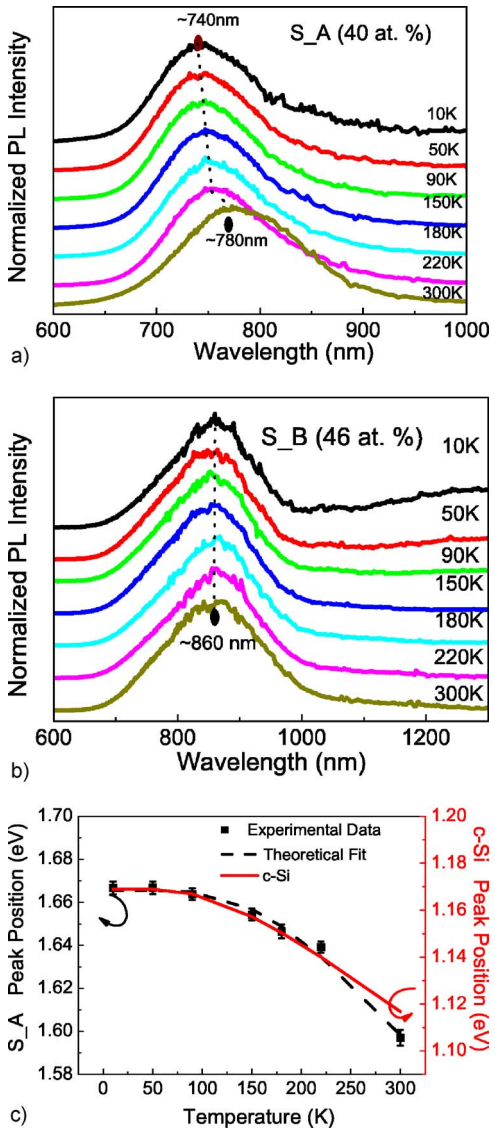

FIG. 5. (Color online) Temperature-dependent PL spectra of samples annealed at 1150 °C for 1 h in N_2 ambient (300 SCCM) with peaks *A* and *B* emission dominant. (a) *S_A* (40 at. % Si); (b) *S_B* (46 at. % Si); (c) PL peak position (eV) of *S_A* as a function of the temperature (full square: ■). The dashed line is the best fit to the experimental data according to Eq. (1). As a comparison, the case of bulk Si is denoted by the solid line.

$$E_{gap}(T) = E_{gap_{,0}} - A \cdot \left(\frac{2}{\exp[\Omega/k_B T] - 1} + 1 \right), \qquad (1)$$

where *A* is the temperature-independent constant (0.064 eV for *c*-Si), k_B is the Boltzmann constant, $E_{gap_{,0}}$ is the energy value at 0 K determined by extrapolation (1.233 eV at 0 K for *c*-Si), and Ω represents an average phonon energy (0.032 eV for *c*-Si). Since light emission from Si NCs in the carrier quantum confinement scheme is due to the band to band radiative recombination of electron-hole pairs confined within nanocrystals,[18] the peak position of *S_A* as a function of temperature should also follow Eq. (1). In order to clearly demonstrate it, a unit conversion of the peak position is performed from wavelength unit (nm) into energy unit (eV). The PL peak position is determined by a parabolic fit near the PL maximum, using the data points greater than 90% of the maximum intensity in Fig. 5(a). The PL peak position of *S_A* as a function of measurement temperature is shown in Fig. 5(c). The error bars in the figure include the testing system error and parabolic fit error. The best fit to the experimental data by Eq. (1) can be achieved with $E_{gap_{,0}} = 1.860 \pm 0.064$ eV, $A = 0.194 \pm 0.065$ eV, and $\Omega = 0.050 \pm 0.007$ eV, presented by the dashed line in Fig. 5(c). As a comparison, the temperature dependence of the *c*-Si band gap is also plotted in Fig. 5(c) by the solid line. Obviously, the observed temperature-induced redshift of *S_A* emission is compatible with the shrinkage of *c*-Si band gap. The increase of the energy gap ($E_{gap_{,0}}$) with respect to *c*-Si is due to the quantum confinement of Si NCs. A similar temperature-dependent PL signal was also reported in SiO/SiO_2 superlattices in Ref. 19 and the breakdown of the *k*-conservation rule for Si NCs was also observed by resonant PL measurements in that case, which further confirms the quantum confinement effect as the origin of the luminescence signal of peak *A*.

Considering *S_B* contains relatively larger Si NCs compared with *S_A*, if the quantum confinement effect makes major contribution to the emission of *S_B*, it's expected that the temperature dependence of the peak position should also follow the behavior described by Eq. (1). However, a negligible shift of the peak position is observed in *S_B*, implying that quantum confined effect is not the origin of peak *B*. Since the position of peak *B* is temperature insensitive, we can conclude that peak *B* is ascribed to the radiative recombination of localized levels formed by interface states between Si NC and the SiO_2 matrix or from defect-related centers in the SiO_2 matrix.[20] The defect-related luminescence in the matrix can be selectively quenched by hydrogen passivation.[20] Therefore, the two types of localized levels can be distinguished by means of postannealing in the forming gas (95% N_2 and 5% H_2) at a relatively low temperature of 500 °C, which has a negligible effect on Si NC size and size distribution due to the lower thermal budget. The observation of PL intensity enhancement in all samples excludes that either peak *A* or *B* is originated from a defect-related recombination in the matrix. Hence, we can unambiguously attribute peak *B* to the interface state recombination.

The enhancement factor of PL integrated intensity after postannealing in the forming gas is presented in Fig. 6. When the dominant emission peak transforms from *A* (Si $\leqslant$42 at. %) to *B* (Si$\geqslant$46 at. %), the enhancement factor of PL intensity increases significantly from 1.5 to 3.5, implying that hydrogen passivation is more effective for enhancing peak *B* emission. The enhancement is generally ascribed to hydrogen passivation of nonradiative P_b centers arising from Si dangling bonds at the Si/SiO_2 interface.[21] Therefore, it has a more significant effect on the radiative emission of interfacial states (peak *B*) than interband transition within Si NCs (peak *A*), again supporting our view on the origins of peaks *A* and *B*.

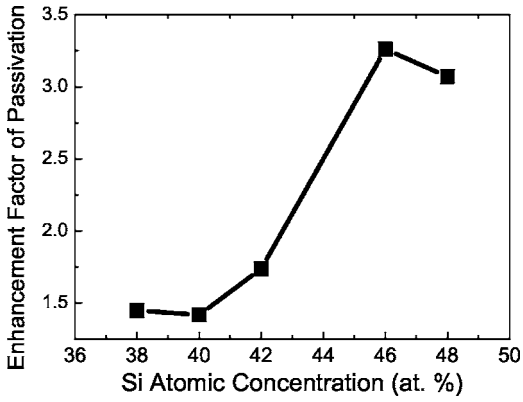

FIG. 6. Enhancement factor of the integrated PL intensity of the samples with different Si concentration after passivation annealing at 500 °C for 1 h in the forming gas of 95% N_2 and 5% H_2. The samples were originally annealed at 1150 °C for 1 h in N_2 ambient (300 SCCM) to form Si NCs before the passivation annealing.

B. Evolution of peaks *A* and *B* under different annealing ambient

In Sec. III A, we observe a transition of dominant emission peak from *A* to *B*, corresponding to a dominant mechanism transition from the quantum confinement effect to the radiative interface state recombination with the increase of Si NC size as a result of higher Si content or annealing at higher temperature. The transition happens in a narrow Si content (42–44 at. %) or annealing temperature (1150–1200 °C) range. These results agree with Qin and Li's theoretical model, i.e., there is a critical NC size, below which the quantum confinement effect dominates, and above which the interface state effect prevails.[12] In the case of annealing at 1150 °C in N_2 ambient, the critical size is estimated to be about 2–2.5 nm based on the information from HRTEM and PL results of samples *S_A* (peak *A* dominated, NC size $=2.0\pm0.3$ nm) and *S_B* (peak *B* dominated, NC size $=2.6\pm0.5$ nm).

Another aspect of Qin and Li's model is that the higher the interface state density, the more beneficial for the interface state recombination process.[12] Recent theoretical calculations and experimental observations indicate that double bonded Si=O significantly reduces the effective optical band gap by creating localized states and pinning the band gap of Si NCs, while single bonded groups (Si-H, Si-N) do not form localized states and have much less influence on the energy band of Si NCs.[22,23] Thus, the density of interface states responsible for peak *B* emission in SRO films is particularly linked to the number of Si=O bonds per unit volume, which can be modified by the annealing environment.[9,24] Figure 7 compares the effect of annealing ambient on the PL spectra of 42 at. % Si sample annealed at 1150 °C. In the inert Ar case, peak *B* makes a major contribution to the PL signal (peak intensity ratio A/B is 0.2). In the flowing O_2 case, the spectrum becomes rather broad, obviously consisting of both *A* and *B* bands (A/B is 0.6). The case of N_2 ambient with lower flow rate (10 SCCM denotes cubic centimeters per minute at STP) is similar to that of O_2, probably due to the residual O_2 in our annealing furnace at

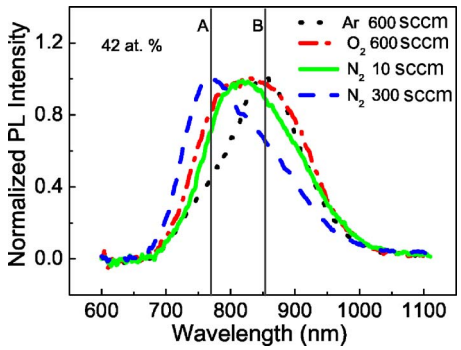

FIG. 7. (Color online) A comparison of PL spectra of 42 at. % Si sample annealed at 1150 °C for 1 h in different annealing atmosphere, Ar (500 SCCM), O_2 (600 SCCM), N_2 (10 SCCM), N_2 (300 SCCM). Two solid vertical lines approximately locate peaks *A* and *B* positions, respectively.

lower N_2 flow rate. However, in the case of N_2 with a higher flow rate (300 SCCM), peak intensity ratio of A/B increases to 1. Compared with the inert Ar case, the increase of peak *A* intensity upon N_2 (300 SCCM) or O_2 annealing can be related to the reduction of the Si NC size by reacting with N_2 or O_2,[9,25] making the quantum confinement effect dominant. It should be noted that peak *A* is relatively stronger and peak *B* is weaker in N_2 ambient (300 SCCM) case with respect to the O_2 case. Considering that annealing gas can modify the surface chemistry of Si NC in addition to reduction of NC size, we presume that the decrease of Si=O bonds fraction by N incorporation in the interfacial shell of Si NC and formation of Si-N bonds[26] would also account for the less contribution of peak *B* emission in the case of N_2 (300 sccm) annealing. The investigation of the effect of the surface chemistry on the dominant PL origin of Si NCs is in progress.

IV. DISCUSSION

We observe in Sec. III that the size and the surface chemistry of Si NCs are two factors affecting the origin of photoluminescence from SRO material system. The increasing dominance of the interface state effect with the increase of Si NC size is in good agreement with Qin and Li's prediction in Ref. 12. As Si content, Si NC size, and the structure of interface states tightly interplay in SRO material system described in this paper, a realistic model of Si NCs embedded in amorphous SiO_2 matrix proposed in Ref. 27 is adopted as a firm theoretical understanding of our observations.

According to this realistic model, the fraction of oxygen-related bonds declines drastically as the Si NC size gets smaller, especially for NCs below 2–2.5 nm.[27] On the other hand, in this size range the critical number of interface states required for interfacial recombination-dominated emission increases dramatically with decreasing NC size based on Qin and Li's calculation.[12] Since the number of interface states is shown theoretically to be proportional to the fraction of oxygen-related bonds,[22] a decline in this fraction due to the decrease of Si NC size would make the number of interface states below the critical value for interfacial effect- domi-

nated emission, resulting in a weaker role of interface state recombination compared with the strong quantum confinement effect. Similarly, as Si NC size becomes larger, the increase of the fraction of oxygen-related bonds and the reduction of the critical value for interfacial effect-dominated emission would make the interface state recombination play a crucial role in the luminescence. Moreover, the modification of surface chemistry of Si NCs by annealing in N_2 ambient can also be explained by the combination of Refs. 12 and 27. The decrease of Si═O bonds fraction by N incorporation in the interfacial shell of Si NCs and consequent formation of Si-N bonds is beneficial for the quantum confinement effect to dominate the PL emission.

Another interesting observation in our study is that the localized levels formed by interface states are also size dependent in this study, i.e., peak *B* emission shifts from ~860 nm towards longer wavelength and then saturates at ~930 nm with the increase of Si NC size as mentioned in Sec III. A. Theoretically, the redshift is also tightly related to the increase of the number of Si═O bonds at the surface[28] as a result of the larger NC size.[27] The calculation in Ref. 28 indicates that the addition of new Si═O bonds reduces the energy gap between localized levels, but the amount of reduction is not linear with the number of the double bonds. The more the Si═O bonds, the more the energy gap reduction, but the reduction rate decreases as the Si═O bonds increase so that a sort of saturation limit occurs in the end. This is very consistent with our experimental observation of peak *B* shift with the increase of Si NC size. Hence, the puzzle of abnormal size-dependent behavior of interface states mentioned in Sec. III A can be explained, and our observation also provides experimental evidence to the theoretical calculation in Ref. 28.

V. CONCLUSIONS

In conclusion, we have separated the interface state recombination effect from the quantum confinement effect in PL signals from the SRO material system. Our observations reveal that the larger the size of Si NCs and the higher the interface states density (in particular Si═O bonds), the more beneficial for the interface state recombination process to surpass the quantum confinement process, in support of Qin and Li's model.[12] The transition trend of the two luminescence mechanisms as a function of Si NC size can be explained based on a realistic model of Si NCs embedded in a SiO_2 matrix.

ACKNOWLEDGMENTS

The authors would like to thank the research engineer J. L. Zhu at the Institute of Semiconductors (China) for thin film fabrication by PECVD, X. P. Zhang at Peking University (China) for HRTEM micrographs, and J. F. Liu at Massachusetts Institute of Technology (USA) for fruitful discussions and earnest revisions of the manuscript. The research project is supported by the State Key Program NSFC No. 60336010 in China.

*Electronic address: wangxiaoxin@red.semi.ac.cn

[1] A. G. Cullis, L. T. Canham, and P. D. J. Calcott, J. Appl. Phys. **82**, 909 (1997).
[2] E. Werwa, A. A. Seraphin, L. A. Chin, C. Zhou, and K. D. Kolenbrander, Appl. Phys. Lett. **64**, 1821 (1994).
[3] H. Morisaki, F. W. Ping, H. Ono, and K. Yazawa, J. Appl. Phys. **70**, 1869 (1991).
[4] S. Hayashi, T. Nagareda, Y. Kanzawa, and K. Yamamoto, Jpn. J. Appl. Phys., Part 1. **32**, 3840 (1993).
[5] T. Shimizu-Iwayama, K. Fujita, S. Nakao, K. Saitoh, T. Fujita, and N. Itoh, J. Appl. Phys. **75**, 7779 (1994).
[6] F. Iacona, G. Franzò, and C. Spinella, J. Appl. Phys. **87**, 1295 (2000).
[7] Y. Kanemitsu, S. Okamoto, M. Otobe, and S. Oda, Phys. Rev. B **55**, R7375 (1997).
[8] S. Okamoto and Y. Kanemitsu, Solid State Commun. **103**, 573 (1997).
[9] J. De la Torre, G. Bremond, A. Souifi, G. Guillot, N. Buffet, and P. Mur, Opt. Mater. **27**, 1004 (2005).
[10] L. Dal Negro, M. Cazzanelli, B. Danese, L. Pavesi, F. Iacona, G. Franzò, and F. Priolo, J. Appl. Phys. **96**, 5747 (2004).
[11] M. V. Wolkin, J. Jorne, P. M. Fauchet, G. Allan, and C. Delerue Phys. Rev. Lett. **82**, 197 (1999).
[12] G. G. Qin, and Y. J. Li, Phys. Rev. B **68**, 85309 (2003).
[13] J. S. Biteen, A. L. Tchebotareva, A. Polman, N. S. Lewis, and H. A. Atwater, Mater. Res. Soc. Symp. Proc. **770**, I6.2.1 (2003).
[14] F. Iacona, C. Bongiorno, C. Spinella, S. Boninelli, and F. Priolo, J. Appl. Phys. **95**, 3723 (2004).
[15] A. T. Voutsas, M. K. Hatalis, J. Boyce, and A. Chiang, J. Appl. Phys. **78**, 6999 (1995).
[16] R. A. Street, Adv. Phys. **25**, 397 (1976).
[17] P. Y. Yu, and M. Cardona, *Fundamentals of Semiconductors* (Springer-Verlag, Berlin, 1996).
[18] C. Delerue, G. Allan, and M. Lannoo, Phys. Rev. B **48**, 11024 (1993).
[19] J. Heitmann, F. Müller, L. Yi, and M. Zacharias, Phys. Rev. B **69**, 195309 (2004).
[20] K. S. Min, K. V. Shcheglov, C. M. Yang, H. A. Atwater, M. L. Brongersma, and A. Polman, Appl. Phys. Lett. **69**, 2033 (1996).
[21] M. López, B. Garrido, C. García, P. Pellegrino, A. Pérez-Rodríguez, J. R. Morante, C. Bonafos, M. Carrada, and A. Claverie, Appl. Phys. Lett. **80**, 1637 (2002).
[22] A. Puzder, A. J. Williamson, J. C. Grossman, and G. Galli, Phys. Rev. Lett. **88**, 097401 (2004).
[23] M. Yang, K. Cho, J. Jhe, S. Seo, J. H. Shin, K. J. Kim, and D. W. Mon, Appl. Phys. Lett. **85**, 3408 (2004).
[24] K. C. Scheer, R. A. Rao, R. Muralidhar, S. Bagchi, J. Conner, C. Perez, M. Sadd, and B. E. White. Jr., J. Appl. Phys. **93**, 5637 (2003).
[25] A. R. Wilkinson and R. G. Elliman, J. Appl. Phys. **96**, 4018 (2004).
[26] V. Mulloni, P. Bellutti, and L. Vanzetti, Surf. Sci. **585**, 137 (2005).
[27] G. Hadjisavvas and P. C. Kelires, Phys. Rev. Lett. **93**, 226104 (2004).
[28] M. Luppi and S. Ossicini, Phys. Rev. B **71**, 035340 (2005).